Journal of Catalysis 369 (2019) 312–323

Contents lists available at ScienceDirect

Journal of Catalysis

journal homepage: www.elsevier.com/locate/jcat

# Modulating the catalytic behavior of non-noble metal nanoparticles by inter-particle interaction for chemoselective hydrogenation of nitroarenes into corresponding azoxy or azo compounds

Lichen Liu, Patricia Concepción, Avelino Corma *

*Instituto de Tecnología Química, Universitat Politècnica de València–Consejo Superior de Investigaciones Científicas (UPV-CSIC), Av. de los Naranjos s/n, 46022 Valencia, Spain*

ARTICLE INFO

*Article history:*
Received 6 September 2018
Revised 31 October 2018
Accepted 8 November 2018
Available online 5 December 2018

*Keywords:*
Ni@C
$CeO_2$
Nitroarenes
Selective hydrogenation
Azoxy
Azo

ABSTRACT

Aromatic azoxy compounds have wide applications and they can be prepared by stoichiometric or catalytic reactions with $H_2O_2$ or $N_2H_4$ starting from anilines or nitroarenes. In this work, we will present the direct chemoselective hydrogenation of nitroarenes with $H_2$ to give aromatic azoxy compounds under base-free mild conditions, with a bifunctional catalytic system formed by Ni nanoparticles covered by a few layers of carbon (Ni@C NPs) and $CeO_2$ nanoparticles. The catalytic performance of Ni@C-$CeO_2$ catalyst surpasses the state-of-art Au/$CeO_2$ catalyst for the direct production of azoxybenzene from nitrobenzene. By means of kinetic and spectroscopic results, a bifunctional mechanism is proposed in which, the hydrogenation of nitrobenzene can be stopped at the formation of azoxybenzene with >95% conversion and >93% selectivity, or can be further driven to the formation of azobenzene with >85% selectivity. By making a bifunctional catalyst with a non-noble metal, one can achieve chemoselective hydrogenation of nitroarenes not only to anilines, but also to corresponding azoxy and azo compounds.


## 1. Introduction

Selecting the desired reaction pathway among several possible is a key objective for heterogeneous catalysis [1–3]. It has been demonstrated in the literature that, by tuning the adsorption properties of molecules on catalyst surface and the formation of reaction intermediates, it is possible to achieve unique chemoselectivities by solid catalysts [4–7]. Moreover, by preparation of multifunctional catalysts, transformations which require multiple steps can be achieved in a one-pot process, leading to process intensification that can reduce the energy consumption and improve the efficiency of the global process [8–10].

Aromatic azoxy compounds are important intermediate compounds with wide application as chemical stabilizers, polymerization inhibitors, dyes, pigments, as well as precursors for materials used in electronic displays and pharmaceuticals [11,12]. Moreover, aromatic azoxy compounds can be further transformed into hydroxyazo compounds through the Wallach rearrangement [13]. Conventionally, aromatic azoxy compounds are prepared by stoichiometric reactions (such as the condensation between hydroxylamine and nitrosobenzene), which is less atom-economic and may produce hazardous by-products [14]. Therefore, in the last decade, some catalytic processes have been developed and aromatic azoxy compounds can be obtained by the oxidative coupling of anilines using metal oxides as catalyst and $H_2O_2$ as the oxidant (Fig. 1a) [15,16]. Aromatic azoxy compounds can also be obtained through the reduction of nitroarenes with hydrazine (see Fig. 1b) [17,18]. Compared with previous processes, these heterogeneous catalytic systems are more efficient and sustainable, but the use of reactants, such as $H_2O_2$ and hydrazine, is still required.

Considering the reaction pathways for hydrogenation of nitroarenes into different products (see Fig. 2), it should be possible to achieve the formation of azoxy and azo products if the reaction goes through the condensation route (shown in Fig. 2). Indeed, in the presence of a base, the intermediates formed during the hydrogenation of nitroarenes can be transformed into azoxy and azo products through the condensation route, as has been reported for the hydrogenation of nitrobenzene to azoxybenzene in the presence of n-butylamine as base and using Rh or Ir as metal catalysts (see Fig. 1c) [19].

In recent years, the development of non-noble metal catalysts as substitutes for noble metal catalysts is emerging in the field of heterogeneous catalysis [20]. For chemoselective hydrogenation reactions, it has been reported that Co-, Fe- and Ni-based catalysts show promising catalytic performances for hydrogenation of nitroarenes to anilines [21–23]. Recently, by studying the reaction mechanism and identification of the active sites, non-noble

* Corresponding author.
*E-mail address:* acorma@itq.upv.es (A. Corma).

https://doi.org/10.1016/j.jcat.2018.11.011
0021-9517/

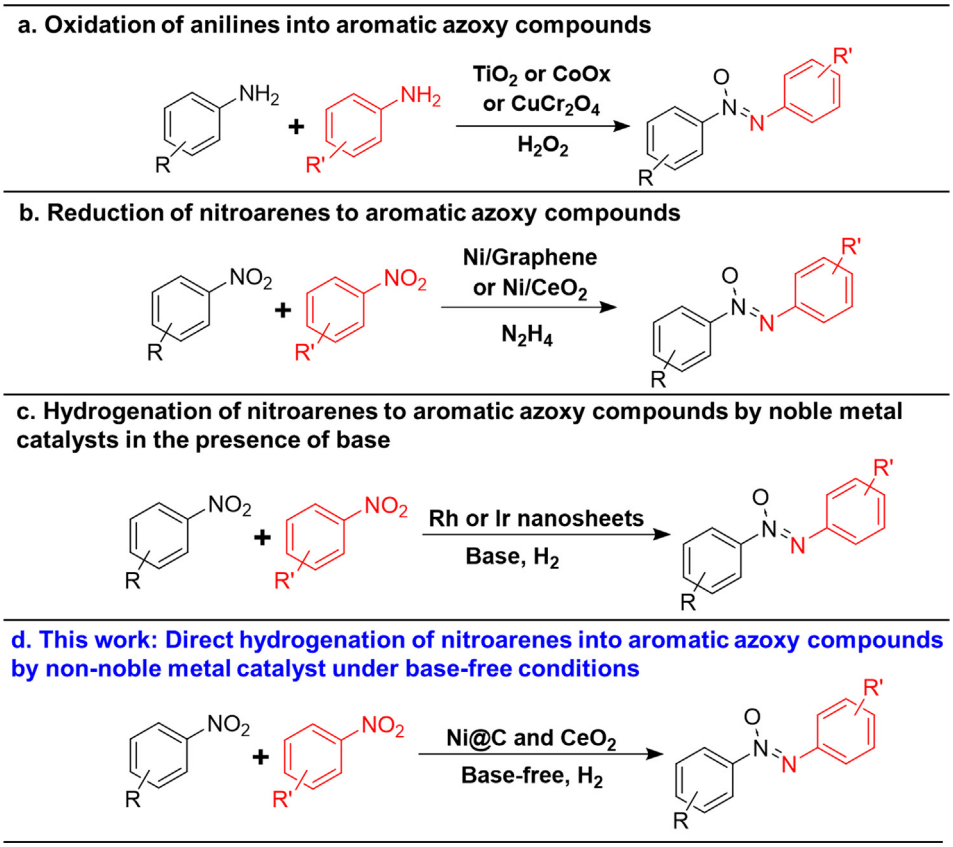


**Fig. 1.** Catalytic routes for the preparation of aromatic azoxy compounds by different approaches, including selective oxidation of anilines with $H_2O_2$ (a), reduction of nitroarenes with $N_2H_4$ (b), hydrogenation of nitroarenes with $H_2$ by noble metal catalysts in the presence of base (c) and direct hydrogenation of nitroarenes with $H_2$ by non-noble metal catalysts under base-free conditions (d).

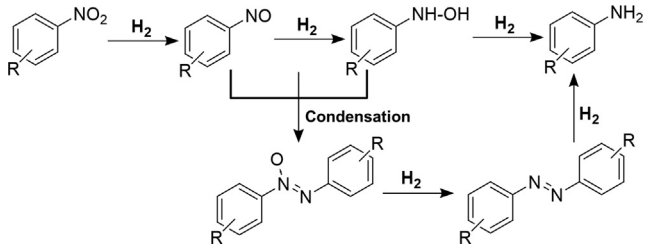


**Fig. 2.** Catalytic hydrogenation of nitroarenes into different products via different routes.

monometallic and bimetallic NPs have been prepared and show better catalytic performance than the state-of-art heterogeneous Au catalysts under the same reaction conditions for chemoselective hydrogenation of nitroarenes to the corresponding anilines [24,25]. It has also been revealed that, the surface structure of the non-noble metal catalysts has significant impact on the selectivity for hydrogenation of nitroarenes [24,26]. Nitrobenzene tends to be hydrogenated directly to aniline on a reduced Ni surface, while nitrosobenzene can be produced as intermediate on a partially reduced Ni surface.

In this work, we show that by combining Ni nanoparticles covered by a few layers of carbon (Ni@C NPs) and $CeO_2$ NPs, a bifunctional catalytic system can be prepared for the direct chemoselective hydrogenation of nitroarenes into corresponding azoxy compounds with high yields under base-free mild conditions. Based on kinetic and spectroscopic studies, we discuss the role of the two components in the Ni@C-$CeO_2$ bifunctional catalyst and how they can interplay. It is of most interest that, based on the nanoparticulate Ni@C catalyst, it is possible to chemoselectively direct the hydrogenation of nitroarenes into corresponding azoxy, azo or aniline products, and we are now able to chemoselectively achieve any of the intermediates involved in the global process of nitroarenes reduction.

## 2. Experiments

$TiO_2$ nanoparticles (from Sigma-Aldrich, product No. 718467-100G), $Al_2O_3$ nanoparticles (from NanoScale NanoActive®, with a surface area of ~300 $m^2/g$), $SiO_2$ nanoparticles (from Sigma-Aldrich, product No. 236772-100G with a surface area of ~480 $m^2/g$), $ZrO_2$ nanoparticles (from Sigma-Aldrich, product No. 544760-5G with a surface area of ~25 $m^2/g$) and $CeO_2$ nanoparticles (from Rhodia with a surface area of ~120 $m^2/g$) were used directly as received without any treatments. Au/$CeO_2$ catalyst with 1 wt% of Au was obtained from Johnson-Matthey and was directly used for the catalytic test without any treatments.

Hydrotalcite (Mg/Al = 4) nanoparticles (with a surface area of ~80 $m^2/g$) were prepared by a precipitation method. 8 mmol of $Mg(NO_3)_2{\cdot}6H_2O$ and 20 mmol of $Al(NO_3)_3{\cdot}9H_2O$ were dissolved in 100 mL of $H_2O$, resulting the formation of solution A. 40 mmol of $Na_2CO_3$ and 200 mmol of NaOH was dissolved in 100 mL of $H_2O$, resulting in the formation of solution B. Solution A was dropped into solution B slowly under vigorous stirring at room temperature. After ~1 h, the mixing of solution A and B was completed and the suspension was aged at 65 °C for ~18 h. The while precipitate was obtained by filtration and washed with $H_2O$. Finally, the solid product was dry in an oven at 100 °C.

### 2.1. Synthesis of the catalysts

#### 2.1.1. Synthesis of Co@C and Ni@C nanoparticles

Co@C and Ni@C nanoparticles were synthesized by a carbon-coating method, which was described in our recent work [25].

$CeO_2$@C nanoparticles were prepared by a similar carbon-coating approach. 1.0 g of $CeO_2$ nanoparticles, 720 mg of glucose and 20 mL distilled water was mixed to a suspension with the help of ultrasonication. The suspension was then transferred to an autoclave and placed in an oven at 175 °C for 18 h. After the hydrothermal treatment, the solid product was collected by filtration and washed with water and acetone. The dried solid was then annealed in flow $N_2$ at 600 °C for 2 h with a ramp rate of 10 °C/min from room temperature to 600 °C. After the high-temperature annealing, the sample was cooled down to room temperature in $N_2$ flow and stored in a glass vial in ambient environment.

#### 2.1.2. Synthesis of Cu@C and Fe@C nanoparticles

We have also prepared Cu@C and Fe@C nanoparticles by the above-mentioned carbon-coating process. However, that method is not applicable to Cu and Fe. Only bulk Cu and Fe (with particle size larger than 1 μm) were obtained. Therefore, Cu@C and Fe@C nanoparticles were synthesized by reducing metal-EDTA complex, as described in our recent work [24]. More specifically, the Cu-EDTA complex were prepared through a hydrothermal process. First, 6.98 g $Cu(NO_3)_2$, 4.47 g $Na_2EDTA$ and 0.96 g NaOH are dissolved in 20 mL $H_2O$. Then, 10 mL methanol was added to the mixed aqueous solution temperature under stirring at room temperature. After the formation of a homogeneous solution, 23 mL of the purple solution was transferred into a 35 mL stainless steel autoclave followed by static hydrothermal processing at 200 °C for 24 h. After cooling to room temperature, the generated precipitates were filtered and washed with deionized water and acetone several times followed by drying at 100 °C in air for 16 h. The obtained complex was denoted as Cu-EDTA. Then, Cu@C NPs were prepared by reduction of Cu-EDTA in $H_2$ (50 mL/min) at 450 °C for 2 h with a ramp rate of 10 °C/min from room temperature to 450 °C. After the $H_2$ reduction process at 450 °C, the sample was cooled down to room temperature in $H_2$ atmosphere. Then the black solid product was stored in a glass vial in ambient environment.

Fe-EDTA complex was prepared by the same method, using Fe $(NO_3)_3{\cdot}9H_2O$ as the precursor.

#### 2.1.3. Synthesis of Ni-$CeO_2$-C nanocomposites

The Ni-$CeO_2$-C nanocomposites can be prepared by the carbon-coating process in the presence of $CeO_2$ nanoparticles. 1.0 g $CeO_2$ nanoparticles, 720 mg of glucose, 0.5 g of Ni precipitate (obtained from the precipitation of $Ni(Ac)_2$ and sodium carbonate in glycol) was mixed with 20 mL water to form a homogeneous suspension with the help of ultrasonication. The suspension was then transferred to an autoclave and placed in an oven at 175 °C for 18 h. After the hydrothermal treatment, the solid product was collected by filtration and washed with water and acetone. The dried solid was then annealed in flow $N_2$ at 600 °C for 2 h with a ramp rate of 10 °C/min from room temperature to 600 °C. After the high-temperature annealing, the sample was cooled down to room temperature in $N_2$ flow and stored in a glass vial in ambient environment.

#### 2.1.4. Synthesis of Ni/$CeO_2$ by wetness impregnation

Ni/$CeO_2$ with 5.0 wt% of Ni supported on $CeO_2$ was prepared by traditional wetness impregnation method. 123 mg of $Ni(NO_3)_2{\cdot}6H_2O$ was dissolved in 20 mL of water and then 0.5 g of $CeO_2$ nanoparticles was added to the solution. The suspension was kept stirring at room temperature for 2 h before removing the water by heating the suspension at 120 °C. After the removal of the solvent, the solid sample was calcined in flow air at 550 °C for 3 h with a ramp rate of 5 °C/min from room temperature to 550 °C. After the calcination in air, the sample was cooled to room temperature and a subsequent reduction treatment by $H_2$ was carried out at 450 °C for 3 h with a ramp rate of 5 °C/min from room temperature to 450 °C. After the reduction treatment, the sample was cooled down to room temperature in $H_2$ flow and stored in a glass vial in ambient environment.

### 2.2. Characterizations

Powder X-ray diffraction (XRD) was performed with a HTPhilips X'Pert MPD diffractometer equipped with a PW3050 goniometer using Cu Kα radiation and a multisampling handler.

Raman spectra were recorded at ambient temperature with a 785 nm HPNIR excitation laser on a Renishaw Raman Spectrometer ("Reflex") equipped with an Olympus microscope and a CCD detector. The laser power on the sample was 15mW and a total of 20 acquisitions were taken for each spectra.

Samples for electron microscopy studies were prepared by dropping the suspension of solid sample in $CH_2Cl_2$ directly onto holey-carbon coated copper grids. All the measurements were performed in a JEOL 2100F microscope operating at 200 kV both in transmission (TEM) and scanning-transmission modes (STEM). STEM images were obtained using a High Angle Annular Dark Field detector (HAADF), which allows Z-contrast imaging.

The amount of exposed surface Ni atoms in the Ni@C catalyst was determined by $H_2$ chemisorption at 100 °C in an ASAP 2010C Micromeritics equipment by extrapolating the total gas uptakes in the adsorption isotherms at zero pressure. Prior to the measurements the sample was reduced under flowing pure $H_2$ at 400 °C. The percentage of exposed Ni atoms in the Ni@C NPs was estimated from the total amount of chemisorbed $H_2$ assuming an adsorption stoichiometry $H_2$/Ni of 1.

The FTIR spectra were collected with a Bruker Vertex 70 spectrometer equipped with a DTGS detector (4 $cm^{-1}$ resolution, 32 scans). An IR cell allowing *in situ* treatments in controlled atmosphere and temperature from 25 to 500 °C has been connected to a vacuum system with gas dosing facility. Self-supporting pellets (ca. 10 mg $cm^{-2}$) were prepared from the sample powders and treated at 200 °C in hydrogen flow (20 mL $min^{-1}$) for 2 h followed by evacuation at $10^{-4}$ mbar at 250 °C for 1 h. In the case of the $CeO_2$ sample only activation under vacuum at 120 °C have been performed. After activation the samples were cooled down to 25 °C under dynamic vacuum conditions followed by nitrobenzene dosing at 1.5 mbar. Once the physically absorbed and/or gas phase nitrobenzene was removed in evacuation at 25 °C, $H_2$ was co-adsorbed at pressures between 0.4 mbar and 40 mbar. The IR spectra were recorded after 35 min at a specific reaction temperature (from 25 to 150 °C). Additional experiments were performed at different reaction times (from 20 min to 180 min) at each temperature. It should be noted that, the IR experimental procedure used in this work is not *operando*. However, the above methodology allows us to obtain information about the intrinsic reactivity of surface sites in the solid catalyst in the presence of the reactant molecule. With these information, it enables us to follow the reaction pathways for the hydrogenation of nitrobenzene and nitrosobenzene on $CeO_2$ and Ni@C-$CeO_2$ catalysts.

X-ray photoelectron spectra of the catalysts were recorded with a SPECS spectrometer equipped with a Phoibos 150MCD-9 multichannel analyzer using non-monochromatic AlKα (1486.6 eV) irradiation. Spectra were recorded using analyser pass energy of 30 eV, an X-ray power of 100 W and under an operating pressure of $10^{-9}$ - mbar. The sample was pre-reduced by $H_2$ in a pre-treatment chamber at 120 or 200 °C and then transferred to analysis chamber for

the XPS measurements. Peak intensities have been calculated after nonlinear Shirley-type background subtraction and corrected by the transmission function of the spectrometer. During data processing of the XPS spectra, binding energy (BE) values were referenced to C1s peak (284.5 eV) for the Ni@C samples and to the Ce3d5/2 peak at 882.8 eV for the Ni@C-$CeO_2$ samples. CasaXPS software has been used for spectra treatment.

### 2.3. Catalytic tests

The chemoselective hydrogenation of nitroarenes was performed in batch reactors. The reactant, internal standard (hexadodecane), solvent (toluene), powder catalyst as well as a magnetic bar were added into the batch reactor. After the reactor was sealed, air was purged out from the reactor by flushing two times with 10 bar of hydrogen. Then the autoclave was pressurized with $H_2$ to the corresponding pressure. The stirring speed is kept at 1100 rpm and the size of the catalyst powder is below 0.05 mm to avoid either external or internal diffusion limitation. Finally, the batch reactor was heated to the target temperature. For the kinetic studies, 50 μL of the mixture was taken out for GC analysis at different reaction times. The products were identified by GC-MS.

In some cases, the catalyst was pre-reduced by $H_2$ at an elevated temperature (150 °C) for a certain time and then cooled down to room temperature. Then nitrobenzene was injected into the batch reactor and the temperature was raised to 120 °C again for the hydrogenation reaction test.

## 3. Results and discussions

Non-noble transition metal nanoparticles covered by thin carbon layers (named as Co@C, Fe@C, Cu@C and Ni@C, respectively) that could, in principle, catalyze the hydrogenation reaction, were prepared according to our recent work (see the experimental details). The morphologies of those as-prepared metal@C nanoparticles have been characterized by TEM. As shown in Fig. 3, Ni NPs show particle size ranging from 5 to 20 nm, with an average size of ~10 nm and those Ni NPs are covered by a few carbon layers (less than 10 layers, mostly around 3–8 layers). Structural characterizations (XRD and Raman) show that the as-prepared sample contains metallic Ni NPs with disorder carbon surrounding them. In the case of Co@C, the morphology is similar to Ni with a slightly larger average particle size of ~15 nm (see Fig. S1). For Cu@C and Fe@C, the particle size is much larger than for Ni@C or Co@C (see Fig. S2).

Firstly, we have studied the catalytic behavior of the several types of non-noble metal NPs that in principle can work as catalysts (Co@C, Ni@C, Fe@C and Cu@C NPs) for hydrogenation of nitrobenzene under mild conditions (120 °C and 10 bar of $H_2$). As shown in Table 1, Fe@C and Cu@C NPs show poor activity for hydrogenation of nitrobenzene while Co@C and Ni@C NPs are sensibly more active. Indeed, the Ni@C sample achieves 42% conversion after 150 min reaction time and gives aniline as the major product (~90% selectivity) with azoxybenzene (~9% selectivity) as byproduct. However, in the case of Co@C, very high selectivity to aniline is observed, though conversion is lower.

Since a small amount of azoxybenzene (9.7% selectivity) and azobenzene (3.2% selectivity) was obtained with Ni@C NPs, this encourages us to study the kinetic profiles for hydrogenation of nitrobenzene on this catalyst, to see the evolution of the different products with reaction time. As shown in Fig. S3, nitrosobenzene can be observed at the starting stage, which comes from a new reaction pathway on Ni nanoparticles, being different to that reported on noble metal catalysts (such as Au, Pt) [26]. The selectivity to nitrosobenzene decreases with reaction time and aniline becomes the major product when conversion is >20%. From these results, it can be speculated that the nitrosobenzene formed as a primary product would be rapidly hydrogenated to aniline and the formation of azoxybenzene would not be kinetically favorable on this catalyst. However, when we reacted nitrosobenzene on Ni@C NPs (see Fig. S4), azoxybenzene was obtained with high yield and aniline only starts to form when the conversion of nitrosobenzene was >90%. Then, according to the reaction network in Fig. 2 and the catalytic results shown in Figs. S3 and S4, a catalyst in which the rate of hydrogenation of nitrosobenzene to aniline is decreased and nitrosobenzene is allowed to accumulate, may allow to produce azoxybenzene (see summary in Fig. S5). In order to achieve high selectivity for hydrogenation of nitrobenzene to azoxybenzene, it would be critical to stabilize the nitrosobenzene and phenylhydroxylamine intermediates, and to react them into azoxybenzene.

Considering that the intermediates (nitrosobenzene and phenylhydroxylamine) in the condensation reaction route (see Fig. 2) can be stabilized and condensed in a basic environment, we thought that the selectivity to the azoxybenzene product should be improved in the presence of a solid catalyst with suitable basicity. After screening a combination of Ni@C and metal oxides with varying acid-base properties (see Table 1), it was found that the combination of Ni@C and $CeO_2$ NPs gives high selectivity to azoxybenzene (94%) at full conversion of nitrobenzene, though $CeO_2$ alone in the absence of Ni@C NPs is not active for this reaction. We have also noticed that, other metal oxides with different acid-base properties such as $Al_2O_3$, $TiO_2$, $SiO_2$ or hydrotalcite (Mg/Al = 4) give much lower selectivity to azoxybenzene.

At this point, we assume that a bifunctional catalyst prepared by supporting Ni on $CeO_2$ NPs should work for the hydrogenation of nitrobenzene to azoxybenzene. Following that assumption, a supported Ni/$CeO_2$ catalyst (with 5 wt% of Ni on $CeO_2$) was prepared by wet impregnation and it was then reduced by $H_2$ at 450 °C and passivated by air at room temperature after the $H_2$ reduction treatment. As it can be seen, the as-prepared Ni/$CeO_2$ catalyst shows poor activity for hydrogenation of nitrobenzene, which is probably caused by the re-oxidation of Ni when exposed to air. Indeed, when the Ni/$CeO_2$ catalyst was reduced in the reactor before the catalytic test, the activity improved significantly while selectivity was preserved, implying that metallic Ni is the active component for hydrogenation of nitroarenes. Hou et al. have studied the chemical states of Ni particles supported on $CeO_2$ [18]. The XPS results show that, only part of the Ni can be reduced by $H_2$ even after treatment at 500 °C. Therefore, at our current reaction temperature (120 °C), only a small amount of Ni (<5%) in the supported Ni/$CeO_2$ catalyst can be reduced (see the XPS results in Fig. S6). The thin carbon layers in the Ni@C NPs can protect Ni from deep oxidation by air and promote the partial reduction of Ni under reaction conditions. Therefore, the Ni@C-$CeO_2$ catalyst in which Ni nanoparticles with a high reduction degree are mixed with $CeO_2$ is more active than the Ni/$CeO_2$ in which only a small part of Ni is reduced.

To figure out the reaction mechanism of Ni@C-$CeO_2$ for direct conversion of nitrobenzene to azoxybenzene, we have performed the following experiments. Firstly, bare $CeO_2$ is not active for hydrogenation of nitrobenzene (see Fig. S7), inferring that the initial activation of nitrobenzene should be related with Ni@C NPs. Afterwards, it is shown in Fig. S8 that nitrosobenzene can be selectively hydrogenated into azoxybenzene by Ni@C-$CeO_2$ with high reaction rate. Furthermore, as shown in Figs. S9 and S10, only hydrogenation of nitrosobenzene was observed during the competitive hydrogenation tests with nitrobenzene and azoxybenzene.

It is found that nitrosobenzene can be directly and selectively converted to azoxybenzene heating the nitrosobenzene in toluene solvent (0.5 mol $L^{-1}$) in the absence of solid catalyst with a

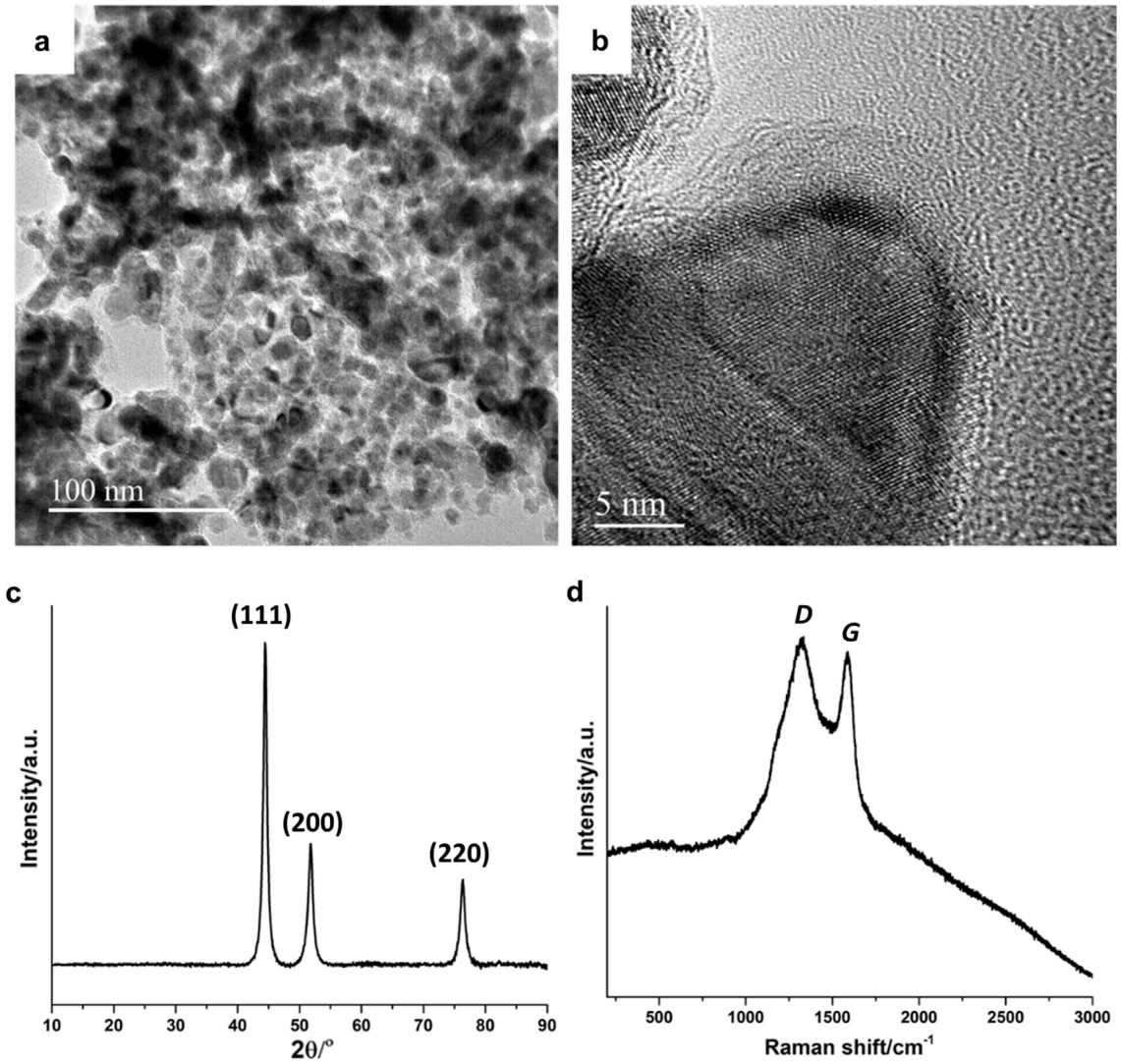


**Fig. 3. Structural characterization of Ni@C nanoparticles.** (a and b) TEM and high-resolution TEM image. (c) XRD pattern of Ni@C nanoparticles, being the typical diffraction pattern of metallic Ni (PDF code:96-210-0650), without peaks corresponding to NiO or other species. (d) Raman spectrum of Ni@C nanoparticles, showing the presence of Raman bands corresponding to ***D*** and ***G*** bands. The ratio between these two bands suggests that, the carbon layers covered on Ni nanoparticles are disordered.

**Table 1**
Catalytic performance of various non-noble metal catalysts for hydrogenation of nitrobenzene.[a]

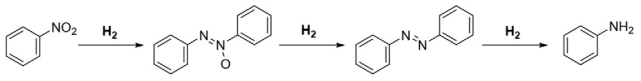


1a 1b 1c 1d

| Entry | Sample | Time/min | Conversion/% | Selectivity to Azoxy (1b) | Selectivity to Azo (1c) | Selectivity to Aniline (1d) |
|---|---|---|---|---|---|---|
| **1** | **Ni@C** | **150** | **43.4** | **9.7** | **3.2** | **85.5** |
| **2** | **Co@C** | 210 | 9.1 | – | – | >99.0 |
| **3** | **Cu@C** | 240 | <3 | – | – | – |
| **4** | **Fe@C** | 240 | <3 | – | – | – |
| **5** | **Ni@C+$CeO_2$** | **50** | **100** | **94.1** | **4.1** | **1.8** |
| **6** | **$CeO_2$** | 300 | <2 | – | – | – |
| **7** | **Ni/$CeO_2$** | 840 | 5.9 | 75.6 | 6.2 | 18.3 |
| **8** | **Ni/$CeO_2$-*in situ* reduced** | 150 | 35.1 | 94.5 | 0.9 | 4.6 |
| **9** | **Ni@C+$Al_2O_3$** | 110 | 83.7 | 10.7 | 5.6 | 83.8 |
| **10** | **Ni@C + $TiO_2$** | 145 | 45.7 | – | 15.9 | 84.1 |
| **11** | **Ni@C+$SiO_2$** | 150 | 44.7 | – | 1.6 | 98.4 |
| **12** | **Ni@C+Hydrotalcite** | 75 | 84.8 | 6.5 | 5.6 | 74.3 |
| **13** | **Co@C+$CeO_2$** | 360 | 13.3 | 77.8 | – | 22.2 |
| **14** | **Cu@C+$CeO_2$** | 360 | <5 | – | – | – |
| **15** | **Fe@C+$CeO_2$** | 360 | <2 | – | – | – |

[a] Reaction conditions: 1 mmol of nitrobenzene, 2 mL toluene as solvent, 120 °C and 10 bar of $H_2$. 1.5 mg of metal nanoparticles and 10 mg of metal oxide as co-catalyst. The yield of different products are calculated based on hexadecane as internal standard. For Ni/$CeO_2$ (containing 5 wt% of Ni), 20 mg of the solid catalyst was used as catalyst.

selectivity of ~90% at > 90% conversion. It should be noted, when using Ni@C+$CeO_2$ as the catalyst for hydrogenation of nitrosobenzene, the initial reaction rate is 4 times faster than the corresponding homogeneous reaction, indicating that Ni@C+$CeO_2$ is catalytically active for the hydrogenation of nitrosobenzene to azoxybenzene.

However, this homogeneous reaction is strongly related to the concentration of nitrosobenzene in the solvent. As shown in Fig. S11, the initial reaction rate decreases significantly when reducing the concentration of nitrosobenzene from 0.5 mol $L^{-1}$ to 0.05 mol $L^{-1}$ and 0.025 mol $L^{-1}$. As we already know, the concentration of nitrosobenzene intermediate produced by Ni@C nanoparticles under our reaction conditions is very low, even lower than 0.025 mol $L^{-1}$ (as we can see in Fig. S12). Therefore, under our reaction conditions for the direct hydrogenation of nitrobenzene to azoxybenzene, the influence of homogeneous reaction is negligible when compared to the catalytic reaction rate by Ni@C-$CeO_2$ catalyst (see Fig. S13).

Since the concentration of nitrosobenzene as intermediate in the reaction mixture can be very low during the hydrogenation of nitrobenzene, we have also carried out a competitive hydrogenation experiment with a mixture of 90% nitrobenzene and 10% of nitrosobenzene at 60 °C. As shown in Fig. S14a, when only Ni@C was used as the catalyst, nitrosobenzene was firstly hydrogenated to both azoxybenzene and aniline while nitrobenzene was not converted until nearly most of the nitrosobenzene was consumed. Indeed, when the conversion of nitrosobenzene reaches ~70%, the hydrogenation of nitrobenzene started to occur, implying a competitive adsorption between nitrosobenzene and nitrobenzene on the surface of Ni@C nanoparticles. When Ni@C-$CeO_2$ was used as the catalyst (see Fig. S14b), nitrosobenzene was also firstly selectively hydrogenated to azoxybenzene with a higher reaction rate and >90% selectivity to azoxybenzene. More importantly, hydrogenation of nitrobenzene only occurs when almost all the nitrosobenzene in the reaction mixture was converted. These results infer that, hydrogenation of nitrobenzene on Ni@C is more preferable when the concentration of nitrosobenzene is low (<0.02 mol $L^{-1}$), and that the presence of $CeO_2$ can accelerate the selective conversion of nitrosobenzene to azoxybenzene, which explains the higher reactivity and selectivity of Ni@C-$CeO_2$. Since nitrosobenzene is not observed as the intermediate when using Ni@C-$CeO_2$ as the catalyst, it implies that nitrosobenzene may be preferentially absorbed by the Ni@C-$CeO_2$ composite catalyst and converted further to azoxybenzene.

On the basis on the above control experiments, it can be deduced that the introduction of $CeO_2$ to Ni@C nanoparticles can selectively adsorb and convert the low-concentration nitrosobenzene rapidly to avoid the over-hydrogenation reaction to aniline on Ni@C nanoparticles. However, for doing that, nitrosobenzene formed on the Ni@C NPs should diffuse and adsorb on the $CeO_2$ NPs or the interfacial sites between Ni@C-$CeO_2$ nanoparticles. For effective hydrogenation of the nitrosobenzene, the $H_2$ activated on the Ni@C NPs should also reach the absorption sites of nitrosobenzene. Then, it will be on the surface of the $CeO_2$ NPs or the Ni@C-$CeO_2$ interfacial sites, where the azoxybenzene is produced. Nevertheless, the presence of Ni@C NPs is key to produce the nitrosobenzene and to activate $H_2$.

Since the model described above requires the diffusion of intermediate products from one catalyst particle to another, mass transportation should be maximized to achieve maximum efficiency. Therefore, we study the influence of stirring speed in the reactor on the rate of reaction. The results presented in Fig. S15 show that the initial reaction rate increases when increasing the stirring rate up to 900 rpm. After that, further increasing the stirring speed has no effects on the initial reaction rate. Nevertheless, in the presence of 10 mg of $CeO_2$, selectivity to azoxybenzene is always high (>95%). To show the influence of stirring rate on the selectivity for azoxybenzene, the amount of $CeO_2$ was decreased to 2 mg, which will cause less contact between Ni@C and $CeO_2$ NPs. The catalytic results presented in Fig. S16 show that the selectivity to azoxybenzene also decreases with the stirring rate, which should be caused by the insufficient diffusion of nitrosobenzene from the Ni@C to $CeO_2$ nanoparticles.

In another experiment, the surface of $CeO_2$ is partially blocked by the carbon coating treatment and then used as the co-catalyst with Ni@C for hydrogenation of nitrobenzene. As can be seen in Fig. S17, the initial reaction rate decreases slightly compared to the naked $CeO_2$. More importantly, the selectivity to azoxybenzene also decreases, which further confirms the participation of $CeO_2$ for achieving high selectivity to azoxybenzene.

To further study the interaction of the reactants and intermediates with the surface of the catalyst, we have also performed the *in situ* IR studies on the $CeO_2$ NPs and Ni@C-$CeO_2$ catalyst. As shown in Fig. 4a, when $CeO_2$ was used alone as catalyst after

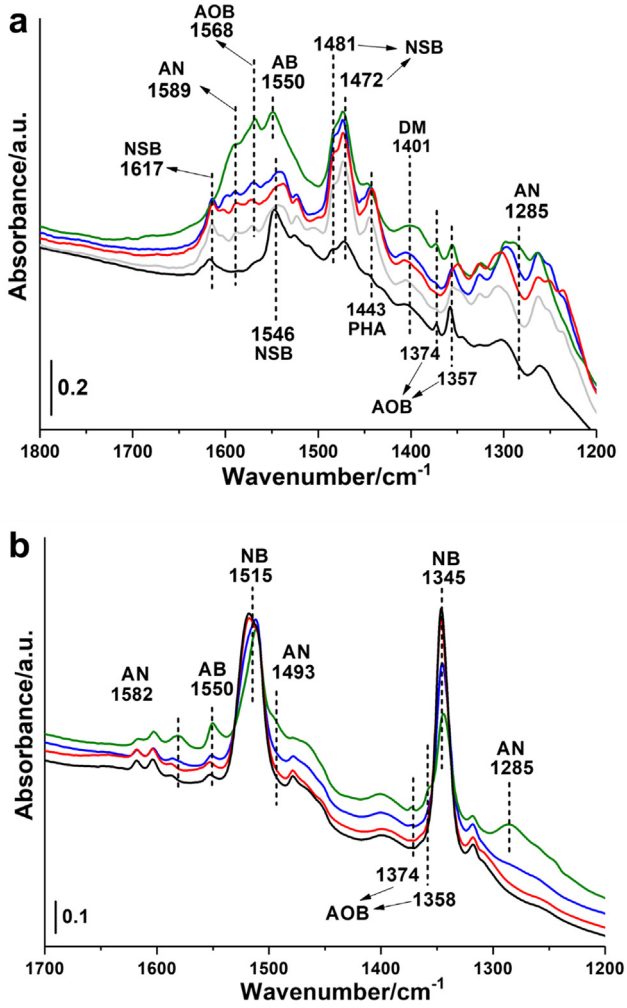


**Fig. 4.** (a) *In situ* IR spectra of hydrogenation of nitrosobenzene (NSB) on $CeO_2$ with 10 mbar $H_2$. Spectra before $H_2$ were collected immediately after NSB dosing (black) and also after 10 min (gray) at 25°. After $H_2$ dosing, spectra were collected at 25 °C (red), 70 °C (blue) and 120 °C (green). (b). *In situ* IR spectra of hydrogenation of nitrobenzene on $CeO_2$ with 10 mbar $H_2$. Before $H_2$ dosing, the spectrum was collected after the introduction of nitrobenzene at 25 °C (black). After $H_2$ dosing IR spectra were collected at 25 °C (red), 70 °C (blue) and 120 °C (green). IR spectra have been acquired after 35 min at each temperature. DM, *cis*-dimer of nitrosobenzene; AN, aniline; AOB, azoxybenzene; AB, azobenzene; PHA, phenylhydroxylamine.

pre-activation in vacuum at 120 °C before the *in situ* IR experiments, nitrosobenzene (1617, 1546, 1481 and 1472 $cm^{-1}$) was adsorbed on $CeO_2$ and the hydrogenation of nitrosobenzene was observed together with the formation of the dimer of nitrosobenzene (1401 $cm^{-1}$) [27] Several reaction products were observed in the IR spectra, including phenylhydroxylamine (1443 $cm^{-1}$), azoxybenzene (1568, 1374 and 1357 $cm^{-1}$), azobenzene (1550 $cm^{-1}$) and aniline (1589, 1285 $cm^{-1}$). Interestingly, the conversion of nitrosobenzene during the *in situ* IR experiments is high, suggesting the activity of $CeO_2$ for hydrogenation reaction [28]. When the reactant was changed to nitrobenzene (1515 and 1345 $cm^{-1}$), the formation of small amounts of azoxybenzene (1374 and 1357 $cm^{-1}$), azobenzene (1550 $cm^{-1}$), and aniline (1582, 1493 and 1285 $cm^{-1}$) was still observed (see Fig. 4b) [29,30]. However, the conversion of nitrobenzene is much lower than that of nitrosobenzene, implying that $CeO_2$ alone is not active enough for hydrogenation of nitrobenzene, probably due to its low activity for $H_2$ activation. Furthermore, the hydrogenation of nitrobenzene and nitrosobenzene on Ni@C-$CeO_2$ has also been followed by *in situ* IR. As shown in Fig. 5, high conversion of nitrosobenzene (1617, 1546, 1481 and 1472 $cm^{-1}$) (Fig. 5a) and nitrobenzene (1515 and 1345 $cm^{-1}$) (Fig. 5b) can be observed together with the formation of the dimer of nitrosobenzene (1401 $cm^{-1}$), azoxybenzene (1572, 1376 and 1357 $cm^{-1}$), azobenzene (1550 $cm^{-1}$), nitrosobenzene (1486 $cm^{-1}$) as well as aniline (1602, 1498 and 1280 $cm^{-1}$) are confirmed according to the IR bands. For comparison, we have also followed the hydrogenation of nitrobenzene on Ni@C + $TiO_2$ catalyst presented above. As can be seen in Fig. S18, only IR bands corresponding to aniline are observed in the IR spectra, which is in line with the catalytic results (see Table 1). The IR results indicate that, nitrosobenzene can be further hydrogenated to phenylhydroxylamine and then form azoxybenzene on $CeO_2$. The role of Ni@C NPs involves the activation of $H_2$ and production of nitrosobenzene as the primary intermediate. As a result of the synergistic effects of Ni@C and $CeO_2$, nitrobenzene can be firstly hydrogenated to nitrosobenzene and then to azoxybenzene.

The pristine Ni@C NPs and the sample after $H_2$ pre-reduction treatment have been measured by XPS. As shown in Fig. S19a, 40.7% of metallic Ni can be observed in the pristine Ni@C NPs. After pre-reduction by $H_2$ at 120 °C, the percentage of metallic Ni increases to 54.2%. Even after pre-reduction treatment at 200 °C, the amount of metallic Ni is 65.6%, suggesting the difficulty to achieve fully reduced Ni nanoparticles under our current reaction conditions for hydrogenation of nitrobenzene in batch reactor. Interestingly, after being physically mixed with $CeO_2$, the amount of metallic Ni in the Ni@C NPs decreases and the NiO species become more difficult to be reduced by $H_2$ (see Fig. S19b). These results refer interaction between Ni@C and $CeO_2$ NPs, which modulates the redox properties of Ni@C NPs. During our catalytic tests, we have observed that, the mixture of Ni@C and $CeO_2$ in the solvent (toluene) can form a magnetic composite. As shown in Fig. S20, after stirring and heating at 60 °C for a short time, the physical mixture of Ni@C and $CeO_2$ was absorbed by the magnetic bar, implying that some interaction may occur between the Ni@C and $CeO_2$ nanoparticles. As a consequence, the non-magnetic $CeO_2$ nanoparticles will also stick to the magnetic bar due to the formation of a nanoparticulate composite with the magnetic Ni@C. There are a number of –OH, –C = O and –COOH groups in the thin carbon layers in the Ni@C NPs, which can interact with the surface of $CeO_2$ nanoparticles. The formation of interfacial contact between Ni@C and $CeO_2$ nanoparticles have been confirmed by TEM-EDS analysis (see Figs. S21–S24).

To further clarify the active sites in Ni@C NPs, we have also pre-reduced the catalyst in the reactor before the hydrogenation reaction and then tested the catalytic behavior of the pre-reduced

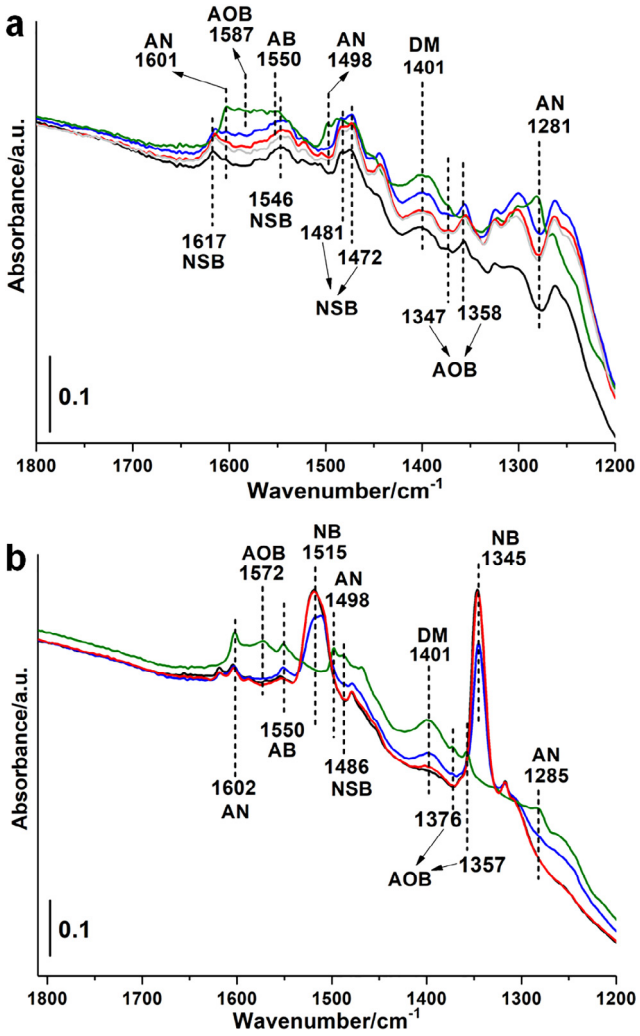


**Fig. 5.** (a) *In situ* IR spectra of hydrogenation of nitrosobenzene on Ni@C + $CeO_2$ with 10 mbar $H_2$. Before the introduction of $H_2$, immediately after NSB dosing at 25° (black) and grey 10 min later). After $H_2$ dosing, the spectra were collected at 25 °C (red), 70 °C (blue) and 120 °C (green). (b) *In situ* IR spectra of hydrogenation of nitrobenzene on Ni@C + $CeO_2$ with 10 mbar $H_2$. Before $H_2$ dosing, spectrum was collected after the introduction of nitrobenzene at 25 °C (black). After $H_2$ dosing, IR spectra were collected at 25 °C (red), 70 °C (blue) and 120 °C (green), respectively. IR spectra have been acquired after 35 min at each temperature. DM, *cis*-dimer of nitrosobenzene; AN, aniline; AOB, azoxybenzene; AB, azobenzene; NB, nitrobenzene; NSB, nitrosobenzene.

catalyst. As shown in Fig. S25, the pre-reduced catalyst shows significantly higher initial activity for hydrogenation of nitrobenzene. More importantly, the high selectivity (>90%) to azoxybenzene is preserved after the pre-reduction treatment. These results indicate that metallic Ni is the active phase in the Ni@C NPs and the NiO present in the Ni@C NPs are not active, but has no influence on the chemoselectivity. Since the Ni@C NPs are not fully reduced under our current conditions (as we discussed before on the XPS results), the nitrosobenzene intermediate formed on Ni@C can be transferred to $CeO_2$. According to our previous work [26], on the fully reduced Ni surface, the nitrosobenzene can be further hydrogenated to aniline directly before the desorption from the surface of Ni@C NPs in the presence of abundant hydrogen.

We have investigated the influence of reaction conditions by *in situ* IR spectroscopy. As displayed in Fig. S26a, when nitrobenzene is co-absorbed with low-pressure $H_2$ (0.4 mbar) on pre-reduced Ni@C-$CeO_2$ catalyst, aniline is not observed. When the

$H_2$ pressure is increased to 10 or 40 mbar (Figs. S26b and c), aniline appears in the IR spectra. By comparing the product distributions in Figs. S16a and S28b, it can be seen that, after pre-reduction treatment, the selectivity to azoxybenzene decreases from ~85% to ~60% when using 1.5 mg of Ni@C and 2 mg of $CeO_2$ as the catalyst for hydrogenation of nitrobenzene. Therefore, the surface properties of Ni@C NPs and their ability for the activation of $H_2$ can also be a factor that influence the product distributions in the hydrogenation of nitrobenzene with bifunctional Ni@C-$CeO_2$ catalyst, although it is not so clear under our current reaction conditions in the batch reactor.

To further prove the role of Ni@C, the hydrogenation of nitrobenzene has been performed with the same amount of $CeO_2$ (20 mg) while varying the amount of Ni@C (0.5–2.5 mg). As presented in Fig. S27, high selectivity to azoxybenzene has been obtained in all the catalytic tests. The initial reaction rate increases when increasing the amount of Ni@C catalyst and the selectivity to azoxybenzene remains high.

The influence of the amount of $CeO_2$ on the catalytic behavior of Ni@C has also been studied. As shown in Fig. S28, addition of just 2 mg of $CeO_2$ as co-catalyst can dramatically improve the activity for hydrogenation of nitrobenzene. The selectivity to azoxybenzene is also improved from <10% to ~60%. Further increasing the amount of $CeO_2$ to 5 mg will lead to >80% selectivity. When 20 mg of $CeO_2$ is used as the co-catalyst, >95% selectivity to azoxybenzene can be achieved.

The above results indicate that at low mass ratios of $CeO_2$/Ni@C (5 mg/1.5 mg), the process for the formation of the azoxybenzene is controlled by the condensation step between the intermediates (nitrosobenzene and phenylhydroxylamine) and reduction step on the $CeO_2$. However, with a higher mass ratio of $CeO_2$/Ni@C (20 mg/2.5 mg), the reaction is controlled by the transformation of nitrobenzene to nitrosobenzene, and reactivity is promoted by increasing the amount of Ni@C. In other words, and as it occurs within any bifunctional catalysts, both components should be optimized to maximize the overall activity and selectivity [31–33].

In conventional supported metal catalysts (such as Au/$TiO_2$, Pt/$TiO_2$, etc.), spectroscopic results and theoretical calculations have proved that nitrobenzene is adsorbed at the metal-oxide interface [34,35]. $H_2$ is activated and dissociated on metal nanoparticles and then transfer to the metal-oxide interface for hydrogenation reaction (see Fig. 6a). In this work, Ni@C interact with $CeO_2$ nanoparticles through inter-particle interaction, which is different to conventional supported metal catalysts.

As we have mentioned before, the evolution of the intermediates during the hydrogenation of nitrobenzene with Ni@C or Ni@C-$CeO_2$ catalyst (as shown in Figs. S3 and S14) indicates that the presence of $CeO_2$ can immediately transform nitrosobenzene into azoxybenzene once nitrosobenzene is formed. Therefore, it is highly likely that, nitrosobenzene can be preferentially absorbed on $CeO_2$. Considering the above catalytic and IR results, we propose that reaction intermediate species and activated $H_2$ are transported not only on a single catalyst particle, but between catalyst particles. As shown in Fig. 6b, **$H_2$** is activated on Ni@C NPs and the activated H species hydrogenate nitrobenzene into nitrosobenzene, which is a rate-limiting step in the reaction. Meanwhile, activated H can transfer to the interfacial sites between Ni@C and $CeO_2$ nanoparticles through inter-particle spillover, and convert nitrosobenzene into phenylhydroxylamine and making the condensation between nitrosobenzene and phenylhydroxylamine for azoxybenzene [36–38]. As discussed before, the interfacial interaction between Ni@C and $CeO_2$ NPs lead to the formation of a Ni@C-$CeO_2$ interface, which facilitate the inter-particle H spillover from Ni@C to $CeO_2$ NPs. Therefore, by employing Ni@C as the active sites for $H_2$ activation and nitrobenzene hydrogenation, and using $CeO_2$ as a co-catalyst for stabilization and further transformation of

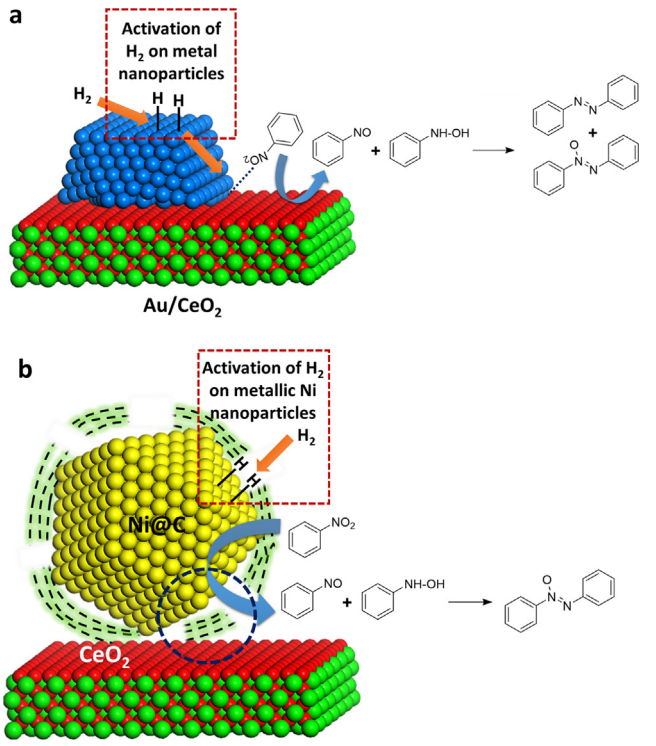


**Fig. 6.** (a) Schematic illustration of direct hydrogenation of nitrobenzene to azoxybenzene and then to azobenzene on Au/$CeO_2$ catalyst. $H_2$ molecules are activated on Au nanoparticles and then transfer to the Au-$CeO_2$ interface to catalyze the hydrogenation of nitrobenzene. Nitrosobenzene and phenylhydroxylamine are the intermediates during the transformation. (b) Schematic illustration of direct chemoselective hydrogenation of nitrobenzene to azoxybenzene with Ni@C-$CeO_2$ catalyst. Interfacial contact is formed between Ni@C and $CeO_2$ nanoparticles under reaction conditions. $H_2$ molecules are activated on Ni@C nanoparticles and then hydrogenate nitrobenzene to nitrosobenzene. The nitrosobenzene intermediate will be preferentially absorbed by the interfacial sites between Ni@C and $CeO_2$ nanoparticles, and further hydrogenated into azoxybenzene.

nitrosobenzene, the direct hydrogenation of nitrobenzene to azoxybenzene can be achieved under base-free mild conditions with high activity and selectivity. The structural of Ni@C-$CeO_2$ bifunctional catalyst based on inter-particulate interaction proposed in this work is different to conventional metal-support catalysts, [39–42] providing a new strategy to design supported metal catalysts.

It should be mentioned that, in the above proposed mechanism, the hydrogenation of nitrobenzene and hydrogenation of nitrosobenzene may occur on two different sites. However, it is also possible that, nitrobenzene is absorbed on $CeO_2$ and then converted into azoxybenzene in the presence of activated H from the Ni@C nanoparticles. According to our above experimental results, we cannot rule out the above possibility. However, considering the results obtained in the mass transfer experiments (see Fig. S16), the intimate contact between Ni@C and $CeO_2$ NPs to form Ni@C-$CeO_2$ interfacial sites is key to achieve high selectivity to azoxybenzene. Thus, we favor the mechanism that involves two separated reactive sites for hydrogenation of nitrobenzene to nitrosobenzene and for the formation of azoxybenzene, respectively.

We have compared the catalytic performance of Ni@C-$CeO_2$ with the state-of-art Au/$CeO_2$ for hydrogenation of nitrobenzene under the same conditions. As shown in Fig. 7, with a higher amount of solid catalyst (50 mg of Au/$CeO_2$ vs. 1.5 mg of Ni@C + 10 mg of $CeO_2$), Au/$CeO_2$ showed a much lower reaction rate. More importantly, Au/$CeO_2$ gives 90% selectivity to azoxybenzene

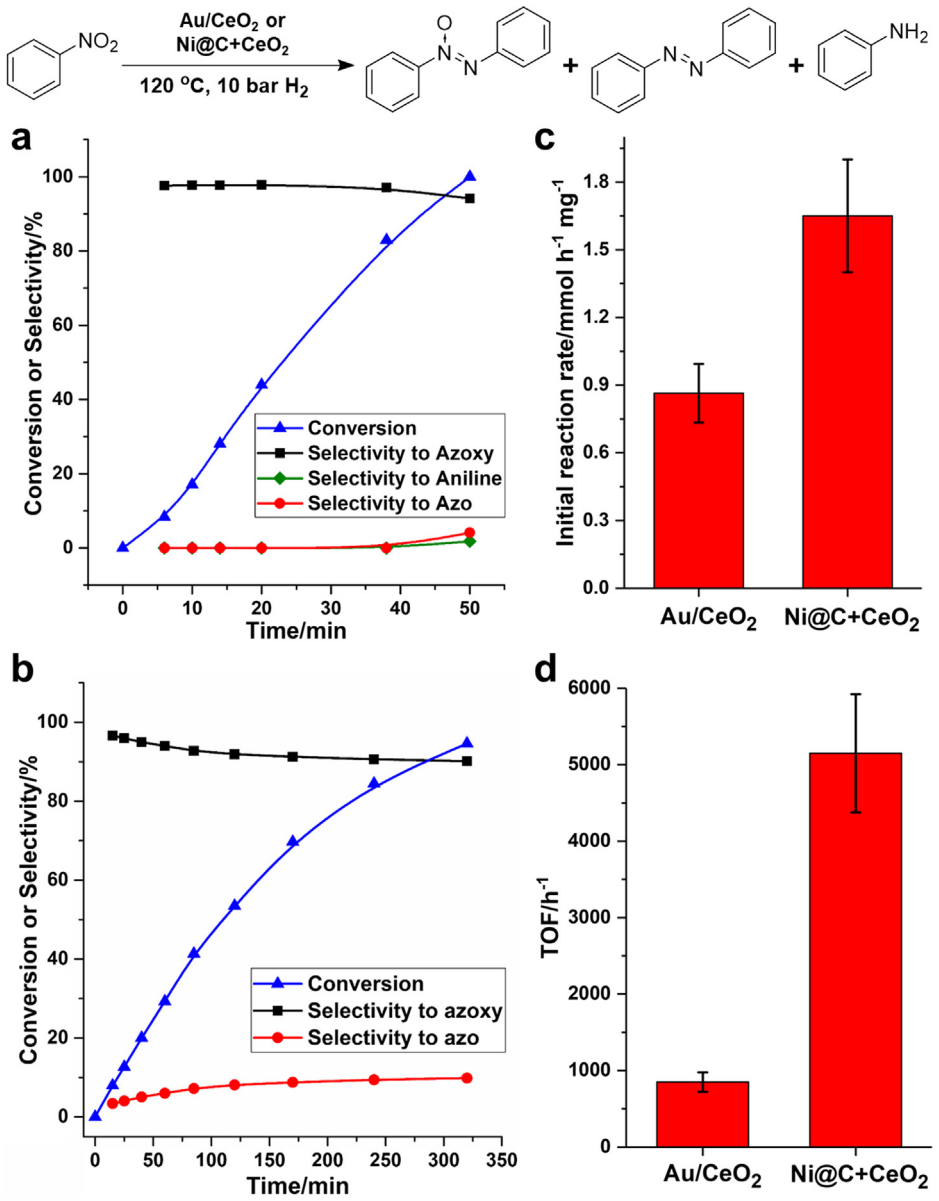


**Fig. 7.** Comparison between $Au/CeO_2$ (1 wt% of Au) and Ni@C-$CeO_2$ for hydrogenation of nitrobenzene under the same conditions. (a) Catalytic result of Ni@C-$CeO_2$ for hydrogenation of nitrobenzene to azoxybenzene. Small amount of azobenzene and aniline were obtained as by-products. Reaction conditions: 1 mmol of nitrobenzene, 2 mL toluene as solvent, 1.5 mg Ni@C and 10 mg of $CeO_2$ as catalyst, 120 °C and 10 bar of $H_2$. (b) Catalytic result of $Au/CeO_2$ for hydrogenation of nitrobenzene. Both azoxybenzene and azobenzene were observed in the products. Reaction conditions: 1 mmol of nitrobenzene, 2 mL toluene as solvent, 50 mg of $Au/CeO_2$ containing 0.5 mg of Au as catalyst, 120 °C and 10 bar of $H_2$. (c) Initial reaction rates ($mmol_{H2}{\cdot}h^{-1}{\cdot}mg^{-1}$) normalized to the mass of metal of $Au/CeO_2$ and Ni@C-$CeO_2$ catalysts for hydrogenation of nitrobenzene. (d) Initial TOF values of $Au/CeO_2$ and Ni@C-$CeO_2$ for hydrogenation of nitrobenzene, calculated based on the surface atoms of Au and Ni in both systems. The amount of surface Au atoms in the $Au/CeO_2$ sample is calculated according to the size distribution of Au nanoparticles. In the case of Ni@C-$CeO_2$ catalyst, the amount of exposed surface Ni atoms is calculated based on the chemisorption measurement using $H_2$ as probe molecules.

at 94% conversion while Ni@C-$CeO_2$ gives 94% selectivity of azoxybenzene at 100% conversion. More importantly, Ni@C-$CeO_2$ catalyst can achieve full conversion of nitrobenzene with a much shorter reaction time than $Au/CeO_2$, especially if considering the lower quantity of solid catalyst used with Ni@C-$CeO_2$. The initial reaction rates normalized to the mass of metal catalysts and the initial turnover frequencies (TOFs) have also been calculated based on the exposed surface atoms in the $Au/CeO_2$ and Ni@C-$CeO_2$ catalysts. Ni@C-$CeO_2$ shows better performance than $Au/CeO_2$, indicating that the combination of Ni@C and $CeO_2$ is a good catalyst for the above-mentioned process.

From a practical point of view, it will be more convenient for the application of this Ni@C-$CeO_2$ bifunctional system if the separated components can be merged into a single solid catalyst. To achieve that aim, we have prepared a Ni-$CeO_2$-C catalyst by one-pot hydrothermal synthesis and post-annealing treatment in $N_2$ at 600 °C (see experimental section for details). As shown in Fig. 8, Ni nanoparticles and $CeO_2$ nanoparticles are mixed together and both of them are covered by a few layers of carbon. The Ni-$CeO_2$-C sample also contains a mixture of metallic Ni and NiO according to the XPS results (see Fig. S29). The catalytic results shown in Table 2 indicate that, Ni-$CeO_2$-C sample is also active and selective for the hydrogenation of nitrobenzene to azoxybenzene. The activity of Ni-$CeO_2$-C is higher than the Ni@C-$CeO_2$ catalyst, which can be attributed the intimate contact between Ni and $CeO_2$ in the Ni-$CeO_2$-C nanocomposites. However, if $CeO_2$ is replaced by other

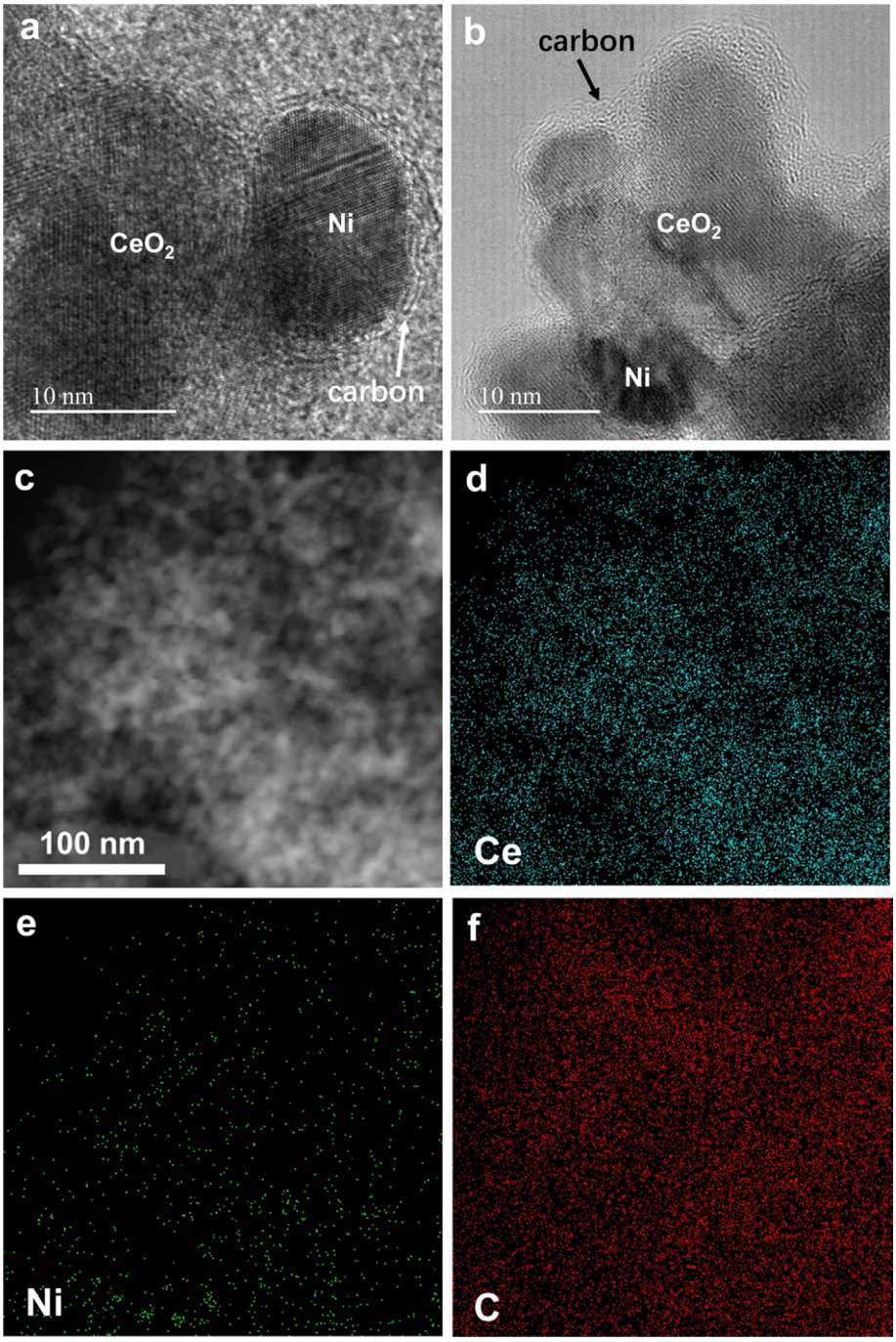


**Fig. 8.** (a and b) High-resolution TEM images of the Ni-$CeO_2$-C catalyst, showing the presence of Ni nanoparticles and $CeO_2$ nanoparticles with thin carbon layers surrounding them. (c–f) STEM image and the corresponding elemental mapping of that area.

**Table 2**
Catalytic performance of Ni-MOx-C catalyst prepared by one-pot hydrothermal synthesis for hydrogenation of nitrobenzene.[a]

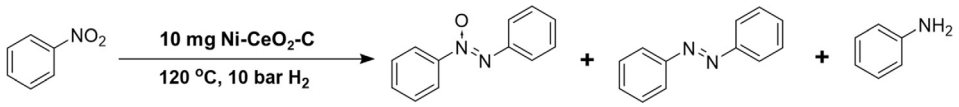


| Sample | Time/min | Conversion/% | Selectivity to Azoxy | Selectivity to aniline | Selectivity to azo |
|---|---|---|---|---|---|
| Ni-$CeO_2$-C | 35 | 97.1 | 92.4 | 4.9 | 2.7 |
| Ni-$TiO_2$-C | 190 | 38.2 | – | >99 | – |
| Ni-$Al_2O_3$-C | 195 | 58.9 | 1.3 | 91.3 | 7.4 |
| Ni-$ZrO_2$-C | 190 | 19.8 | 21.9 | 78.1 | – |

[a] Reaction conditions: 1 mmol of nitrobenzene, 2 mL toluene as solvent, 120 °C and 10 bar of $H_2$. 10 mg of solid catalyst. The amount of Ni in the Ni-MOx-C catalysts is ca. 15 wt%. The yield of different products are calculated based on hexadecane as internal standard.

metal oxides ($TiO_2$, $Al_2O_3$ and $ZrO_2$), the selectivity to azoxybenzene drops dramatically, which is similar to the results obtained before with separated Ni@C and metal oxides.

We have also studied the scope for direct hydrogenation of nitroarenes into corresponding azoxy compounds. As shown in Table 3, high selectivity can be achieved for a variety of nitroarenes with different functional groups. Notably, 3-iodonitrobenzene can be selectivity hydrogenated into corresponding azoxy compounds, which cannot be achieved by supported Au catalysts. Therefore, the combination of Ni@C NPs and $CeO_2$ can catalyze the formation of azoxy compounds with high chemoselectivity by direct hydrogenation of nitroarenes under mild conditions.

According to the reaction scheme shown in Fig. 2, azoxybenzene could be further hydrogenated into azobenzene by simply controlling the reaction time, which offers the possibility to obtain either the corresponding azoxy or azo compounds [29,43]. Then, after achieving high yield of azoxybenzene from nitrobenzene with Ni@C-$CeO_2$ catalyst, the hydrogenation reaction was continued and to our delight, azobenzene can be obtained with yield of 87%. Moreover, we have also studied the scope of Ni@C-$CeO_2$ catalyst for direct hydrogenation of various nitroarenes into corresponding azo compounds, through the azoxy compounds as intermediates. As shown in Table 4, several substituted azo compounds can be obtained from moderate to good yields under bass-free mild conditions [44]. Especially, it is possible to prepare aromatic azo compounds with iodo-substituted group with Ni@C-$CeO_2$ catalyst,

**Table 3**
Scope study on direct hydrogenation of nitroarenes into corresponding aromatic azoxy products.[a]

| Reactant | Product | Yield/% |
|---|---|---|
| 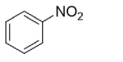 | 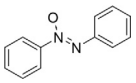 | 94% |
| 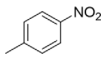 | 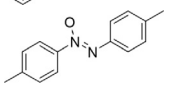 | 88% |
| 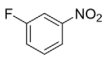 | 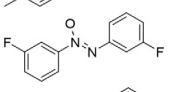 | 95% |
| 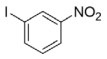 | 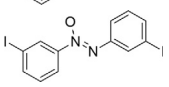 | 92% |
|  | 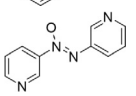 | 91% |
| 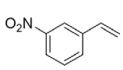 | 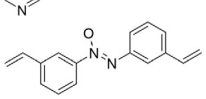 | 58% |
| 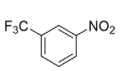 | 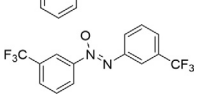 | 98% |
| 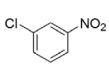 | 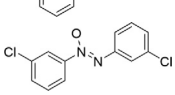 | 92% |
| 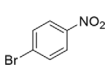 | 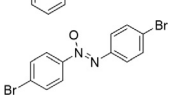 | 84% |
| 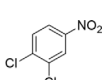 | 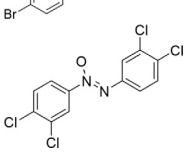 | 88% |

[a] Reaction conditions: 1 mmol of nitrobenzene, 2 mL toluene as solvent, 120 °C and 10 bar of $H_2$. 2.0 mg of Ni@C nanoparticles and 20 mg of $CeO_2$ as co-catalyst. The yield of different products are calculated based on hexadecane as internal standard.

**Table 4**
Scope study on direct hydrogenation of nitroarenes into corresponding azo compounds.[a]

| Reactant | Product | Yield/% |
|---|---|---|
| 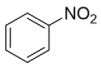 | 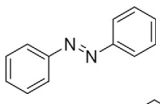 | 87% |
| 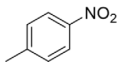 | 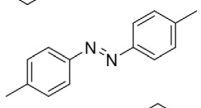 | 68% |
| 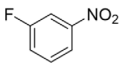 | 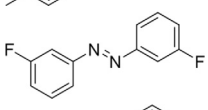 | 58% |
| 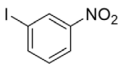 | 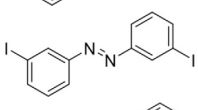 | 62% |
| 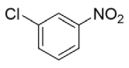 | 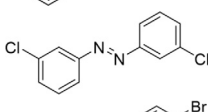 | 91% |
| 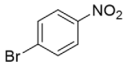 | 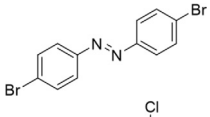 | 71% |
| 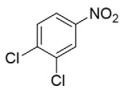 | 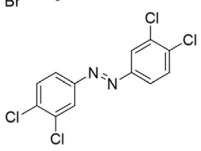 | 70% |

[a] Reaction conditions: 1 mmol of nitrobenzene, 2 mL toluene as solvent, 90 °C and 10 bar of $H_2$. 2.0 mg of Ni@C nanoparticles and 20 mg of $CeO_2$ as co-catalyst. The yield of different products are calculated based on hexadecane as internal standard.

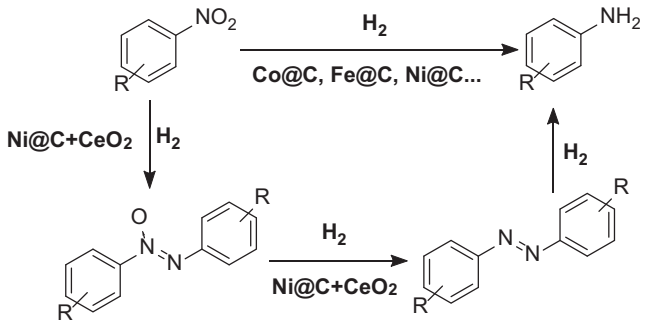


**Fig. 9.** Chemoselective hydrogenation of nitroarenes to different products with non-noble metal catalysts. By choosing different catalysts and co-catalysts, it is possible to obtain various products (azoxy, azo and aniline) by tuning the reaction conditions and reaction time.

which is not possible with Au-based catalysts. At this point, based on the above results and taking into consideration of the high reactivity and low cost of Ni@C-$CeO_2$ catalyst, this catalyst can be a promising substitute for Au/$CeO_2$. At present, combining the results shown in this work and our previous works, we are able to selectively convert nitroarenes into either aniline, azoxy or azo compounds by means of nanoparticulate non-noble metal catalysts (see Fig. 9) [21–25].

## 4. Conclusions

Bifunctional non-noble Ni@C-$CeO_2$ catalysts are found to be highly active and chemoselective catalysts for direct hydrogenation

of nitroarenes into corresponding azoxy or azo products under mild conditions. Notably, the Ni@C-$CeO_2$ catalyst surpasses the performance of state-of-art Au/$CeO_2$ catalyst for direct transformation of nitroarenes to azoxy compounds. Nitroarenes can be reduced to corresponding nitroso compound on Ni@C nanoparticles then diffuse to interfacial sites between Ni@C and $CeO_2$ nanoparticles. $H_2$ is also activated on Ni@C NPs and transfer to the interfacial sites where the chemoselective hydrogenation of nitrosobenzene to azoxybenzene occurs. The Ni@C-$CeO_2$ catalyst enables us to select the product to be obtained (azoxy, azo or aniline compound). Considering the hydrogenation mechanism proposed in this work, it could be possible to tune the catalytic properties of metal nanoparticles by different combinations of metal-oxide(or other co-catalysts) for various chemoselective hydrogenation reactions.

## Acknowledgments

This work has been supported by the European Union through the SynCatMatch project (ERC-AdG-2014-671093). Financial supports by the Spanish Government-MINECO through the program "Severo Ochoa" (SEV-2016-0683) are gratefully acknowledged. The authors also thank the Microscopy Service of UPV for kind help with TEM and STEM measurements.

## Appendix A. Supplementary material

Supplementary data to this article can be found online at https://doi.org/10.1016/j.jcat.2018.11.011.

## References

[1] A. Corma, Heterogeneous catalysis: understanding for designing, and designing for applications, Angew. Chem. Int. Ed. 55 (2016) 6112–6113.
[2] R. Ye, T.J. Hurlburt, K. Sabyrov, S. Alayoglu, G.A. Somorjai, Molecular catalysis science: perspective on unifying the fields of catalysis, Proc. Natl. Acad. Sci. USA 113 (2016) 5159–5166.
[3] R. Schlogl, Heterogeneous catalysis, Angew. Chem. Int. Ed. 54 (2015) 3465–3520.
[4] P. Serna, A. Corma, Transforming nano metal nonselective particulates into chemoselective catalysts for hydrogenation of substituted nitrobenzenes, ACS Catal. 5 (2015) 7114–7121.
[5] M. Filice, J.M. Palomo, Cascade reactions catalyzed by bionanostructures, ACS Catal. 4 (2014) 1588–1598.
[6] M.J. Climent, A. Corma, S. Iborra, M.J. Sabater, Heterogeneous catalysis for tandem reactions, ACS Catal. 4 (2014) 870–891.
[7] G. Szőllősi, Asymmetric one-pot reactions using heterogeneous chemical catalysis: recent steps towards sustainable processes, Catal. Sci. Technol. 8 (2018) 389–422.
[8] B.H. Lipshutz, N.A. Isley, J.C. Fennewald, E.D. Slack, On the way towards greener transition-metal-catalyzed processes as quantified by E factors, Angew. Chem. Int. Ed. 52 (2013) 10952–10958.
[9] R.A. Sheldon, The E factor 25 years on: the rise of green chemistry and sustainability, Green Chem. 19 (2017) 18–43.
[10] A. Leyva-Perez, P. Garcia-Garcia, A. Corma, Multisite organic-inorganic hybrid catalysts for the direct sustainable synthesis of GABAergic drugs, Angew. Chem. Int. Ed. 53 (2014) 8687–8690.
[11] H.E. Bigelow, Azoxy compounds, Chem. Rev. 9 (1931) 117–167.
[12] M.M. Russew, S. Hecht, Photoswitches: from molecules to materials, Adv. Mater. 22 (2010) 3348–3360.
[13] E. Buncel, Catalysis in strongly acidic media and the wallach rearrangement, Acc. Chem. Res. 8 (1975) 132–139.
[14] S. Sakaue, T. Tsubakino, Y. Nishiyama, Y. Ishii, Oxidation of aromatic amines with hydrogen peroxide catalyzed by cetylpyridinium heteropolyoxometalates, J. Org. Chem. 58 (1993) 3633–3638.
[15] S.S. Acharyya, S. Ghosh, R. Bal, Catalytic oxidation of aniline to azoxybenzene over $CuCr_2O_4$ spinel nanoparticle catalyst, ACS Sustain. Chem. Eng. 2 (2014) 584–589.
[16] H. Tumma, N. Nagaraju, K.V. Reddy, Titanium (IV) oxide, an efficient and structure-sensitive heterogeneous catalyst for the preparation of azoxybenzenes in the presence of hydrogen peroxide, Appl. Catal. A: Gen. 353 (2009) 54–60.
[17] M.N. Pahalagedara, L.R. Pahalagedara, J. He, R. Miao, B. Gottlieb, D. Rathnayake, S.L. Suib, Room temperature selective reduction of nitrobenzene to azoxybenzene over magnetically separable urchin-like Ni/Graphene nanocomposites, J. Catal. 336 (2016) 41–48.
[18] T. Hou, Y. Wang, J. Zhang, M. Li, J. Lu, M. Heggen, C. Sievers, F. Wang, Peculiar hydrogenation reactivity of Ni–$Ni^{\delta+}$ clusters stabilized by ceria in reducing nitrobenzene to azoxybenzene, J. Catal. 353 (2017) 107–115.
[19] Z.P. Zhang, X.Y. Wang, K. Yuan, W. Zhu, T. Zhang, Y.H. Wang, J. Ke, X.Y. Zheng, C.H. Yan, Y.W. Zhang, Free-standing iridium and rhodium-based hierarchically-coiled ultrathin nanosheets for highly selective reduction of nitrobenzene to azoxybenzene under ambient conditions, Nanoscale 8 (2016) 15744–15752.
[20] L. Liu, A. Corma, Metal catalysts for heterogeneous catalysis: from single atoms to nanoclusters and nanoparticles, Chem. Rev. 118 (2018) 4981–5079.
[21] F.A. Westerhaus, R.V. Jagadeesh, G. Wienhofer, M.M. Pohl, J. Radnik, A.E. Surkus, J. Rabeah, K. Junge, H. Junge, M. Nielsen, A. Bruckner, M. Beller, Heterogenized cobalt oxide catalysts for nitroarene reduction by pyrolysis of molecularly defined complexes, Nat. Chem. 5 (2013) 537–543.
[22] R.V. Jagadeesh, A.E. Surkus, H. Junge, M.M. Pohl, J. Radnik, J. Rabeah, H. Huan, V. Schunemann, A. Bruckner, M. Beller, Nanoscale $Fe_2O_3$-based catalysts for selective hydrogenation of nitroarenes to anilines, Science 342 (2013) 1073–1076.
[23] G. Hahn, J.-K. Ewert, C. Denner, D. Tilgner, R. Kempe, A reusable mesoporous nickel nanocomposite catalyst for the selective hydrogenation of nitroarenes in the presence of sensitive functional groups, ChemCatChem 8 (2016) 2461–2465.
[24] L. Liu, P. Concepción, A. Corma, Non-noble metal catalysts for hydrogenation: a facile method for preparing Co nanoparticles covered with thin layered carbon, J. Catal. 340 (2016) 1–9.
[25] L. Liu, F. Gao, P. Concepción, A. Corma, A new strategy to transform mono and bimetallic non-noble metal nanoparticles into highly active and chemoselective hydrogenation catalysts, J. Catal. 350 (2017) 218–225.
[26] R. Millán, L. Liu, M. Boronat, A. Corma, A new molecular pathway allows the chemoselective reduction of nitroaromatics on non-noble metal catalysts, J. Catal. 364 (2018) 19–30.
[27] S. Meijers, V. Ponec, J. Catal. 160 (1996) 1–9.
[28] G. Vile, B. Bridier, J. Wichert, J. Perez-Ramirez, Ceria in hydrogenation catalysis: high selectivity in the conversion of alkynes to olefins, Angew. Chem. Int. Ed. 51 (2012) 8620–8623.
[29] D. Combita, P. Concepción, A. Corma, Gold catalysts for the synthesis of aromatic azocompounds from nitroaromatics in one step, J. Catal. 311 (2014) 339–349.
[30] G. Richner, J.A. van Bokhoven, Y.M. Neuhold, M. Makosch, K. Hungerbuhler, In situ infrared monitoring of the solid/liquid catalyst interface during the three-phase hydrogenation of nitrobenzene over nanosized Au on $TiO_2$, Phys. Chem. Chem. Phys. 13 (2011) 12463–12471.
[31] F. Jiao, J. Li, X. Pan, J. Xiao, H. Li, H. Ma, M. Wei, Y. Pan, Z. Zhou, M. Li, S. Miao, J. Li, Y. Zhu, D. Xiao, T. He, J. Yang, F. Qi, Q. Fu, X. Bao, Selective conversion of syngas to light olefins, Science 351 (2016) 1065–1068.
[32] J. Zecevic, G. Vanbutsele, K.P. de Jong, J.A. Martens, Nanoscale intimacy in bifunctional catalysts for selective conversion of hydrocarbons, Nature 528 (2015) 245–248.
[33] X. Kong, Y. Zhu, H. Zheng, X. Li, Y. Zhu, Y.-W. Li, Ni Nanoparticles inlaid Nickel phyllosilicate as a metal-acid bifunctional catalyst for low-temperature hydrogenolysis reactions, ACS Catal. 5 (2015) 5914–5920.
[34] M. Boronat, P. Concepcion, A. Corma, S. Gonzalez, F. Illas, P. Serna, A Molecular mechanism for the chemoselective hydrogenation of substituted nitroaromatics with nanoparticles of gold on $TiO_2$ catalysts: a cooperative effect between gold and the support, J. Am. Chem. Soc. 129 (2007) 16230–16237.
[35] A. Corma, P. Serna, P. Concepcion, J.J. Calvino, Transforming nonselective into chemoselective metal catalysts for the hydrogenation of substituted nitroaromatics, J. Am. Chem. Soc. 130 (2008) 8748–8753.
[36] R. Prins, Hydrogen spillover. Facts and fiction, Chem. Rev. 112 (2012) 2714–2738.
[37] S. Lee, K. Lee, J. Im, H. Kim, M. Choi, Revisiting hydrogen spillover in Pt/LTA: Effects of physical diluents having different acid site distributions, J. Catal. 325 (2015) 26–34.
[38] W. Karim, C. Spreafico, A. Kleibert, J. Gobrecht, J. VandeVondele, Y. Ekinci, J.A. van Bokhoven, Catalyst support effects on hydrogen spillover, Nature 541 (2017) 68–71.
[39] L. Liu, X. Gu, Y. Cao, X. Yao, L. Zhang, C. Tang, F. Gao, L. Dong, Crystal-plane effects on the catalytic properties of Au/$TiO_2$, ACS Catal. 3 (2013) 2768–2775.
[40] L. Liu, C. Ge, W. Zou, X. Gu, F. Gao, L. Dong, Phys. Chem. Chem. Phys. 17 (2015) 5133–5140.
[41] D.I. Enache, J.K. Edwards, P. Landon, B. Solsona-Espriu, A.F. Carley, A.A. Herzing, M. Watanabe, C.J. Kiely, D.W. Knight, G.J. Hutchings, Solvent-free oxidation of primary alcohols to aldehydes using Au-Pd/$TiO_2$ catalysts, Science 311 (2006) 362–365.
[42] M. Cargnello, V.V. Doan-Nguyen, T.R. Gordon, R.E. Diaz, E.A. Stach, R.J. Gorte, P. Fornasiero, C.B. Murray, Control of metal nanocrystal size reveals metal-support interface role for ceria catalysts, Science 341 (2013) 771–773.
[43] X. Liu, H.Q. Li, S. Ye, Y.M. Liu, H.Y. He, Y. Cao, Gold-catalyzed direct hydrogenative coupling of nitroarenes to synthesize aromatic azo compounds, Angew. Chem. Int. Ed. 53 (2014) 7624–7628.
[44] W. Liu, L. Zhang, W. Yan, X. Liu, X. Yang, S. Miao, W. Wang, A. Wang, T. Zhang, Single-atom dispersed Co–N–C catalyst: structure identification and performance for hydrogenative coupling of nitroarenes, Chem. Sci. 7 (2016) 5758–5764.